*European Journal of Soil Science*, June 2006, **57,** 287–294 doi: 10.1111/j.1365-2389.2005.00737.x

# Tracing sediment dynamics and sources in eroding rills with rare earth elements

T. W. LEI[a], Q. W. ZHANG[a], J. ZHAO[a] & M. A. NEARING[b]
[a]*State Key Laboratory of Soil Erosion and Dryland Farming on the Loess Plateau, Institute of Soil and Water Conservation, CAS and MWR, Yangling, Shaanxi 712100, China, and* [b]*USDA-ARS Southwest Watershed Research Center, Tucson, AZ 85719, USA*

**Summary**

Eroding rills evolve morphologically in time and space. Most current studies on rill erosion use spatially averaged soil erosion data, providing little information on soil erosion dynamics. A method is proposed to use rare earth elements (REEs) to trace sediment distribution in eroding rills. Laboratory flume simulation experiments were conducted at three flow rates (2, 4 and 8 litres minute$^{-1}$) and five slope gradients (5, 10, 15, 20 and 25°) with three replicates of each treatment. The rills, of 8 m length, were subdivided into 10 equal segments of 0.8 m length and 0.1 m width, with a different REE applied to each segment. We derived computational formulae for estimating the distribution of eroded amounts along the rills. The actual erosion distribution along rills was then estimated with the data from the experiments. The precision of the REEs for tracing rill erosion was analysed. The results showed that sediment concentration increased with rill length, but the increased rate (the slope of the curve) flattened gradually. Sediment yields increased with slope gradients and flow rates, but the slope gradients had a greater effect on sediment concentration than flow rates, and greater flow rates caused more rill erosion and soil loss under the same slope gradient. The results also demonstrated the feasibility of using REEs to trace the dynamic processes of rill erosion.

## Introduction

Most current soil loss data are spatially and temporally averaged, though various techniques are available to measure spatially distributed erosion. The information about temporal and spatial variation of soil loss is useful for developing and validating soil erosion prediction models, understanding the mechanism of soil erosion, assessing the on-site and off-site impacts of soil and water loss, and finding the best solutions to control soil erosion efficiently.

Under steady concentrated flow into a well-defined (uniform slope with no variation in width) rill channel, the relationship between sediment concentration ($c$) in rill flow and the rill length ($x$) was conceptually and numerically illustrated by Huang *et al.* (1996) and Lei *et al.* (1998), respectively, as:

$$c = A(1 - \exp(-\beta x)), \tag{1}$$

where $A$ ($> 0$) and $\beta$ ($> 0$) are regression coefficients, varying with soil and hydraulic conditions.

Correspondence: T. W. Lei, The Key Laboratory of Modern Precision Agriculture System Integration Research, China Agricultural University, Beijing 100083, China. E-mail: ddragon@public3.bta.net.cn
Received 18 November 2003; revised version accepted 5 April 2005

Equation (1) indicates that sediment concentration increases with rill length and approaches a maximum value of $A$, the sediment concentration at transport capacity. Lei *et al.* (2001) conducted a series of laboratory experiments to verify the sedimentation processes. In their experiments, well-defined rill segments of different lengths were used to yield the sediment concentration as a function of rill length. The method they used is referred to as a traditional or conventional method in this paper. Equation (1) also clearly indicates that the increase in sediment concentration, that is $dc/dx$, decreases exponentially with rill length as:

$$\frac{dc}{dx} = -\beta A \exp(-\beta x). \tag{2}$$

This incremental reduction in sediment concentration is due to a decrease in soil detachment rate. This phenomenon of detachment rate reduction of sediment-loaded flow has been experimentally demonstrated by Lei *et al.* (2002).

Typical existing methods in soil erosion research for measuring soil loss include runoff-plot experiments, watershed monitoring, three-dimensional photography, and laboratory and field rainfall simulation, among others (Tang, 2004). These methods estimate soil erosion as a temporally and spatially integrated quantity by comparing the eroded state after rainfall with the initial soil state, or by collecting eroded

materials. In runoff experiments, one measures runoff and erosion changes with time, but erosion is difficult to measure spatially. Though useful data are obtained, little is quantified about what is actually happening within the eroding area during the course of erosion. Many attempts have been made to use tracers to obtain spatially distributed erosion data.

Ritchie & McHenry (1990) and Walling & He (1999) used bomb-produced $^{137}Cs$ (half-life of 30 years) and Wallbrink & Murray (1993) used naturally occurring $^{210}Pb$ (half-life of 20.2 years) to estimate long-term soil erosion rates and distributions of eroded material across a landscape. However, these methods are quantitatively challenged by inconsistencies and uncertainties. For instance, the estimated soil erosion rates at given $^{137}Cs$ depletion concentrations can differ by more than one order of magnitude (Walling & Quine, 1990). Further, the $^{137}Cs$ and $^{210}Pb$ methods provide no information on sediment origin to determine the erosion process. Wooldridge (1965) and Toth & Alderfer (1960) tried $^{56}Fe$ and $^{60}Co$ for soil erosion tracing. These radioactive elements can be deliberately applied to study soil erosion. A main problem associated with this type of tracer is the radiological risk to users and the environment. Due to lack of analytical sensitivity, large application rates of the isotopes are normally needed to trace soil erosion and sediment movement.

It is commonly believed that the ideal tracers for the study of soil erosion and sediment sources have to have the following characteristics: they should (i) be strongly bound to soil particles or easily incorporated into aggregates; (ii) not interfere with sediment transportation; (iii) be easy and inexpensive to measure; (iv) have small background concentration in soils; (v) not be easily taken up by plants; and (vi) be environmentally friendly (Riebe, 1995; Zhang *et al*., 2001). Rare earth elements (REEs) are a group of metallic elements, which include scandium, yttrium, and the lanthanide group, that all have similar physiochemical properties. These elements are good candidates for sediment source studies, since they all have the basic characteristics mentioned above, though some are relatively more expensive and some are cheaper. The REE oxides, as industrial products, insoluble in water and other basic solvents, and in powder form, have been tried and used in soil erosion research (Tian *et al*., 1992; Riebe, 1995; Plante *et al*., 1999; Zhang *et al*., 2001). Tian (1997) used rare earth oxides by mixing their powders with soils to identify sediment sources, and transport and deposition of eroded soil particles in a small watershed. Zhang *et al*. (2001) evaluated the feasibility of using REE oxides as tracers for soil erosion studies by examining their binding ability with soil materials. Their results demonstrated the great potential of using REEs in the study of soil erosion mechanisms and sediment transport processes.

This potential of REEs for soil erosion tracing was demonstrated in laboratory flume experiments by Zhang *et al*. (2003) and Polyakov & Nearing (2004). In these studies, REEs were incorporated into soil in a 2 m × 4 m soil box, which was then subjected to simulated rainfall. The results indicated that the REEs were effective for identifying the relative source areas of the sediment within the box, with relatively little problem with sediment size sorting during the transport of the sediment. For the silty, loess-derived soils used in these experiments the REEs bound effectively across the entire range of sediment size distributions, which is an important point for effective sediment tracing. Polyakov *et al*. (2004) developed the laboratory studies into a field study in a small watershed in Ohio, USA, and demonstrated the effectiveness of the tracers for field application.

To understand the dynamic rill erosion process, Lei & Nearing (2000) tried a series of laboratory experiments, in which a flume 8 m long and 0.6 m wide was subdivided into 1/1, 1/2, 1/4 and 1/8 of the total flume length, to measure sediment yield from different rill lengths. However, the rills were not well formed, and their widths fluctuated randomly both spatially and temporally. Lei *et al*. (2001) used very narrow flume strips, 0.1 m wide, to form relatively well-defined rills. They ran rill erosion experiments at flume lengths of 0.5, 1, 2, ..., 7 and 8 m to measure sediment yield from these different rill lengths, in order to trace the rill erosion processes. Whether the erosion processes as detected from these interrupted rills are the same as those from a continuous rill has to be verified with another method. As yet, we have found no reports of the use of REEs for tracing the dynamic processes of rill erosion.

The objectives of this study were: (i) to develop a method for estimating soil erosion in different segments of a rill; (ii) to use the REE tracing method to determine sediment distribution in eroding rills; (iii) to check the rill erosion process as obtained with the experiments using interrupted rill lengths; and (iv) to investigate rill erosion processes as influenced by slope gradient and flow rate.

## Materials and methods

### *Selected REEs and their application*

The following 10 REE oxides were selected for our study: $Ho_2O_3$, $Tb_4O_7$, $Eu_2O_3$, $Yb_2O_3$, $Dy_2O_3$, $Sm_2O_3$, $La_2O_3$, $Tm_2O_3$, $CeO_2$ and $Nd_2O_3$. The rill erosion experiments were conducted in the laboratory using rills 8 m long, subdivided into 10 segments of 0.8 m. Each segment was treated with one of the 10 REE oxides; the application locations of the REE oxides on the slope are shown in Figure 1 and Table 1. Relevant background information on the properties of the REEs is presented in Table 1. The REE series were numbered 1 through 10 from the lower to the upper parts of the rill.

The application depth of the tracers should be deeper than the erosion depth in the rill. Based on previous laboratory experiments, we know that the erosion depth in the upper portion of a rill will be greater than that at the lower part. The results of Lei *et al*. (2002) and Merten *et al*. (2001) showed

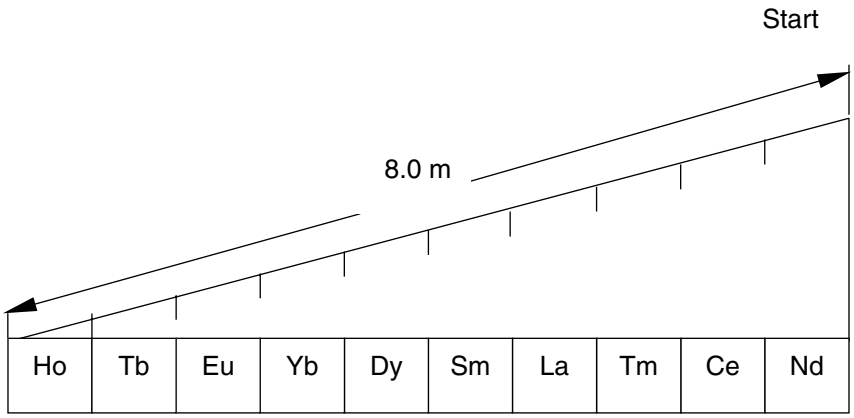


**Figure 1** The application locations of 10 REEs along the rill slope.

that the detachment rate, as indicated by Equation (1), and hence the detached depth along a rill decreased exponentially for a constant flow rate. Therefore, the depth of mixing of the REEs was varied along the slope (Table 1), and REE oxides of lower cost were applied to the top sections of the slopes, where erosion is greater and where more REEs are needed, to reduce costs.

The application concentration in the $i$th segment of the rill, $C_i$ (mg kg$^{-1}$), and total application mass, $A_i$ (g), are listed in Table 1. These values were chosen to be great enough to allow detection of the REE in the eroded soil material. The applied concentration (the difference between total concentration in the eroded material, $c_i$, and the background concentration, $C_i^0$, given in Table 1) was made to be at least twice that of the background value of the REE in the original soil material, for the case where all the soil was eroded.

### *Preparation of the soil materials*

A silt loam, loess-derived soil from Ansai Agricultural Experiment Station on the Loess Plateau of China (109°20′E, 36°50′N) was used in the experiments. The soil texture was 15.9% clay (< 0.005 mm), 63.9% silt (0.005–0.05 mm) and 20.2% sand (> 0.05 mm). The soil material was taken from the top 1 m depth of a sparsely vegetated grass slope. The soil, with a pH value of 8.5, contains 97.3 g kg$^{-1}$ $CaCO_3$, and 4.01 g kg$^{-1}$ organic matter. The soil was air-dried before passing through a sieve of 10 mm aperture for the experiments.

The REE oxides were mixed with sufficient soil to fill the targeted soil layer depth (Table 1). To ensure complete mixing, REE oxides were first mixed well with a small amount of the dried soil and then with the total soil for the layer.

### *Experimental flume*

A laboratory flume of 1 m × 8 m was subdivided into 10 rills of 0.1 m × 8 m with upright PVC boards. The flume and the rill beds were adjustable to allow for experiments on different slopes. Loess soil was glued on to the sides of the PVC boards, with the intention of obtaining a similar roughness on the boards as on the soil surface to minimize the possible impacts of the boards on the water flow. The bottom 30 cm of the flume was packed with the soil to act as a non-erodible layer. Then, the flume was packed loosely and evenly to a depth of

**Table 1** Basic information, soil background concentrations, and application information for each of the REEs

| Rare earth oxide | Atomic symbol | Atomic number | Soil background concentration /mg kg$^{-1}$ | Section number | Application depth /cm | REE application concentration, $C_i$ /mg kg$^{-1}$ | REE application amount, $A_i$ /g |
|---|---|---|---|---|---|---|---|
| $Ho_2O_3$ | Ho | 67 | 1.20 | 1 | 10 | 47.04 | 22.31 |
| $Tb_4O_7$ | Tb | 65 | 0.81 | 2 | 5 | 66.53 | 16.20 |
| $Eu_2O_3$ | Eu | 63 | 1.14 | 3 | 5 | 100.13 | 24.00 |
| $Yb_2O_3$ | Yb | 70 | 2.64 | 4 | 5 | 224.00 | 52.80 |
| $Dy_2O_3$ | Dy | 66 | 4.13 | 5 | 5 | 323.27 | 76.80 |
| $Sm_2O_3$ | Sm | 62 | 5.80 | 6 | 10 | 199.97 | 96.00 |
| $La_2O_3$ | La | 57 | 35.40 | 7 | 10 | 781.95 | 384.00 |
| $Tm_2O_3$ | Tm | 69 | 2.40 | 8 | 10 | 47.25 | 22.34 |
| $CeO_2$ | Ce | 58 | 66.10 | 9 | 15 | 757.65 | 577.97 |
| $Nd_2O_3$ | Nd | 60 | 31.10 | 10 | 15 | 127.77 | 92.55 |

20 cm and to a bulk density of approximately 1.2 g $cm^{-3}$. The soil near the flume walls was slightly higher than the soil surface in the middle in order to minimize the walls' influence on the erosion process. The soil surface was covered with a thin gauze cloth and water was sprayed over the cloth until the soil was saturated with water. The saturated soil was allowed to equilibrate for 24 hours before each run to provide a uniform initial water content and uniform packing.

*Experimental procedures and computations*

Five slopes (5°, 10°, 15°, 20°, 25°), three flow rates (2, 4, 8 litres $minute^{-1}$) and three replicates of each treatment were used in the experiments. Water was applied at the soil surface through an outlet pipe of 50 mm diameter and 9 cm length, drilled evenly with four holes of 0.8 cm diameter on each of four rows, and the water outlet was covered with gauze to ensure minimal disturbance or local scouring of the soil surface at the entrance section. The velocity of the water flow was measured with a dye-tracing technique (Abrahams *et al.*, 1986), with appropriate correction for conversion from leading edge to average velocities. Each experiment was run for a very short time, from 3 to 5 minutes depending on the flow rate and the slope steepness, to collect sufficient eroded materials. The greater the flow rate and the slope, the shorter the running time. All the sediment from each experiment was collected to determine the total eroded amount by the oven-drying method. Part of the eroded materials (at least 5 g, which is required by the analysis method) was taken for REE determination to measure erosion from different sections of the rill.

Three 5-g samples of the original soil (without REE oxide application) were used to determine the background values of the REEs in the soil by means of neutron activation analysis (NAA). The REE oxide concentrations in the eroded sediment and the REE concentration in three 5-g samples of the soil mixed with REE oxides were also measured using NAA.

All the eroded soil was collected and the total erosion and REE concentrations, $c_i$ ($i = 1, 2, \ldots, 10$), of the sediment were measured. The difference between measured $c_i$ and its corresponding background value, $C_i^0$ (kg $kg^{-1}$), multiplied by the total soil erosion, $W$ (kg), determined the eroded amount of the applied REE, $e_i$ (kg, or g for convenience):

$$e_i = \left(c_i - C_i^{\,0}\right) W. \tag{3}$$

The eroded amount of applied REE, $e_i$, is also the product of the amount of soil eroded ($W_i$) from the section where the individual $REE_i$ was applied at the concentration $C_i$ (kg $kg^{-1}$):

$$e_i = W_i C_i. \tag{4}$$

From Equation (4), the amount of soil eroded ($W_i$, kg) from each segment is given as

$$W_i = \frac{e_i}{C_i}. \tag{5}$$

Thus, the amount of soil eroded, $W_i$, from the section where $REE_i$ was applied is the product of the total erosion, $W$, and the ratio of the increased concentration ($c_i - C_i^0$) of $REE_i$ in the eroded material over the applied concentration $C_i$:

$$W_i = \frac{(c_i - C_i^{\,0})}{C_i} W. \tag{6}$$

*Calculation of sediment concentration along the rill*

Assuming that the time of each experimental run is $\Delta T$ (s), the flow rate, $q$ ($m^3$ $s^{-1}$) is stable, and the concentration of sediment contributed from the section of REE, $\lambda$, is constant with time $t$, then $\lambda_i$ may be calculated as follows. Since the erosion from section $i$ on the slope is:

$$W_i = \int_0^{\Delta T} \lambda_i q \mathrm{d}t = \lambda_i q \Delta T, \tag{7}$$

it follows that the sediment concentration contributed from any section, $i$, is

$$\lambda_i = \frac{W_i}{q \Delta T}. \tag{8}$$

From the section furthest from the inflow (section $i = 1$) to the upper section of the slope (section $i = 10$), the sediment concentration at the end of section $i$ is $\theta_i$ (kg $m^{-3}$) and is the sum of the total amount of soil eroded from all the sections above it (i.e. upstream) divided by the total water volume, calculated as:

$$\theta_i = \sum_{j=i}^{10} \lambda_j = \frac{1}{q \Delta T} \sum_{j=i}^{10} W_j \ (i = 1, 2, \cdots, 10). \tag{9}$$

## Results and discussion

*Dynamic sediment distribution along the rills*

The sediment concentration distributions along the rill under different hydraulic conditions, calculated using Equation (9), are presented in Figure 2. Sediment concentration increased rapidly with an increase in rill length, but the rate (the slope of the curve) diminished gradually with the distance downslope. The sediment concentration approached a final stable value towards the end of the rill.

The sediment concentrations at the rill outlets (Figure 2) showed the influence of slope gradient and flow rate on the dynamic sediment distributions in rill erosion. From this figure, it can be seen that as slope increases, the sediment concentrations in the runoff increase, but the rates of increase become smaller. The change for 25° slope was reduced compared with those at slopes < 20°, i.e. the increase in slope gradient induces greater sediment concentration in the flow, but the rate of increase gradually decreases and approaches a stable level.

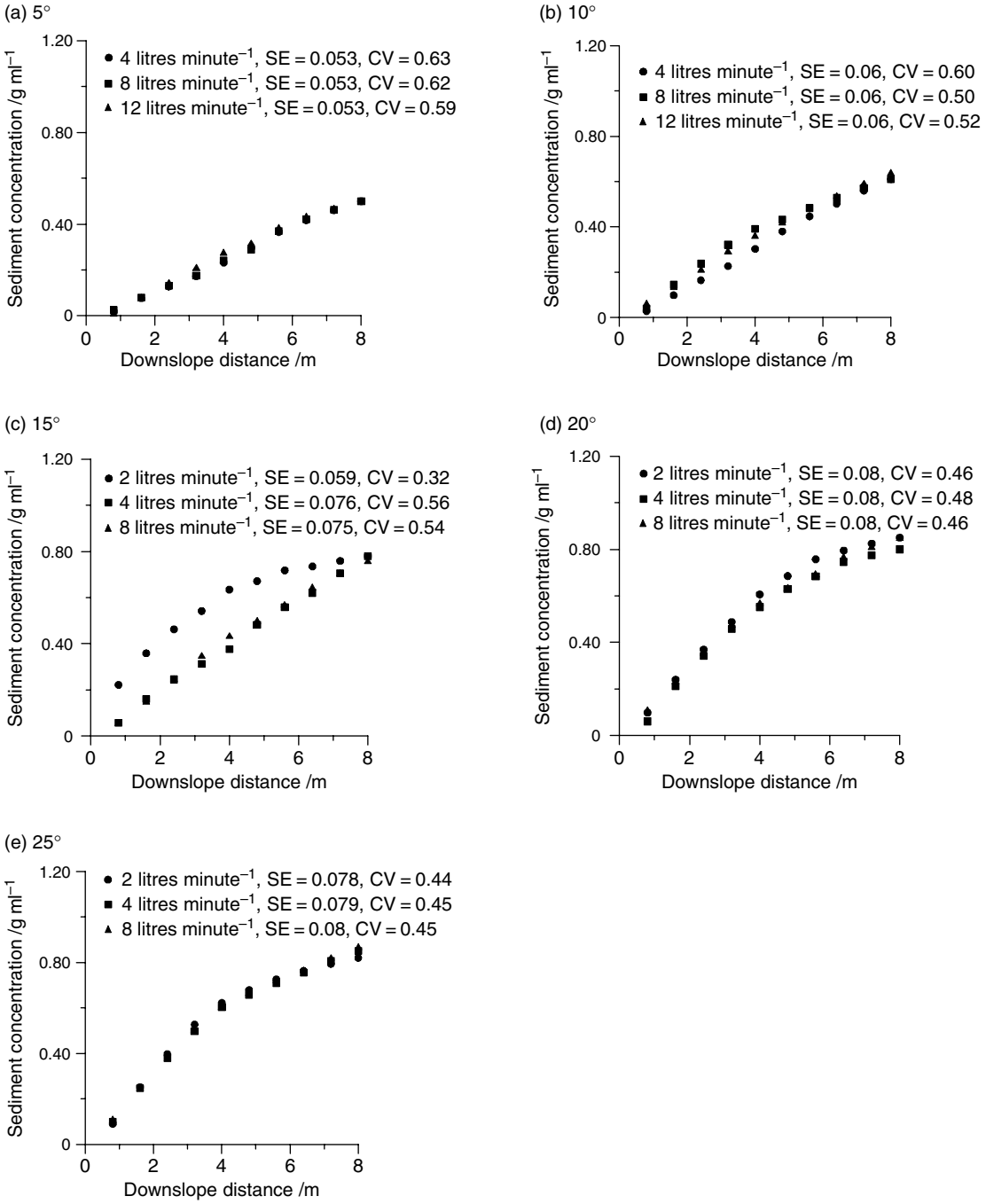


**Figure 2** Sediment concentration distributions along the rills at the different slopes and flow rates: (a) 5°, (b) 10°, (c) 15°, (d) 20°, and (e) 25° slopes.

Figure 2 also indicates that, under a given slope gradient, the sediment concentrations under different flow rates followed almost the same curve, and the sediment concentrations at the rill outlets were about the same for different flow rates. This implies that the slope gradient had a greater effect on sediment concentration than flow rate. As soil loss, or sediment load, is the product of sediment concentration and flow rate, the greater flow rate with (about) the same sediment concentration delivers proportionally more sediment. This means the greater the flow rate, the greater the erosion and the more severe the soil loss, i.e. greater flow rates cause more severe rill erosion. This could be because under that same slope gradient, the greater the flow rate, the greater the velocity of the water flow which induces more detachment of soil particles from the rill bed. Further, at greater flow rates, although the flow velocity increases to some extent, either the rill is cut

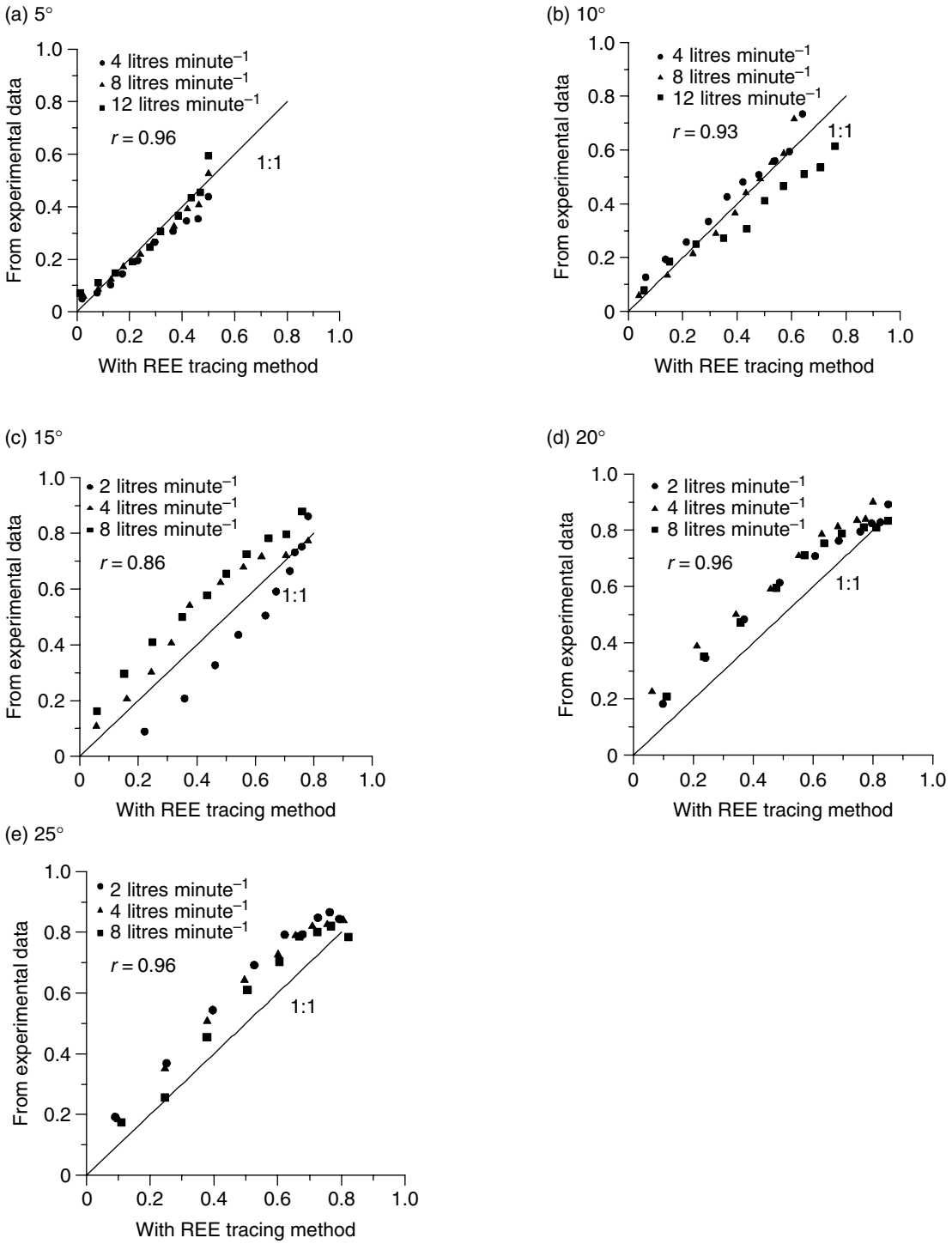


**Figure 3** Comparison of the sediment concentration distributions obtained with the REE method and those obtained with the different rill length method: (a) 5°, (b) 10°, (c) 15°, (d) 20°, and (e) 25° slopes.

deeper or the flow width becomes larger. Thus, the wetted perimeter increases with flow rate, which increases the area for soil detachment, which in turn contributes more sediment to the water flow. For the soil used in the experiments, the combined influences of the increased flow velocity and the extended wetted perimeter as caused by greater flow rate increased rill erosion to make the sediment concentrations almost the same under different flow rates.

Measurement accuracy of the REE method was determined as the relative error between the total soil erosion estimated

(the summary of $W_i$) with the REE tracing method and the total eroded soil material collected ($W$) as:

$$\delta = \left( \sum_{i=1}^{10} W_i \Big/ W - 1 \right) \times 100\% \,, \qquad (10)$$

where $\delta$ (%) is the relative error and $i$ is the section number for the different REEs applied. All relative errors calculated under the experimental conditions were less than 15%.

### *Comparison of the distribution of sediment concentration from the REE method and those from previous experiments*

Lei *et al.* (2001) measured the spatial changes of rill erosion with laboratory flume experiments by using different rill lengths for each experimental run, under the assumption that the incremental change in erosion rate from the longer rill would correspond with the additional flume length. The data in Figure 3 show that the results from the REE tracing method agree well with those from the previous experimental data. The good correlations between the two groups of data were shown by the large correlation coefficients ($r$) (Figure 3). A $t$-test determined that the significance levels ($\alpha$) were 4.5, 9.7, 8, 5.7 and 2.5% for the 5°, 10°, 15°, 20° and 25° slope gradients, respectively. The sediment concentrations at the flume outlet, as measured by Lei *et al.* (2001) with different rill lengths, and those as summed from each segment with the REE method under different flow rates and slope gradients are compared in Figure 4. The two groups of data agree well, with a large correlation coefficient ($r = 0.99$, $\alpha = 2.1\%$) and a regression coefficient close to one (1.035). This indicates the precision of the REE method for tracing the rill erosion process. The REE method represents the actual rill erosion process and can serve as a basis for checking the rationale of the experimental procedures for studying the rill erosion process with different rill lengths. The advantage of the REE method is that it takes measurements of the continuous rill sedimentation process with one sampling attempt, while the experiments with different rill lengths were done under the assumption that each experimental run under different rill lengths follows the same sedimentation process.

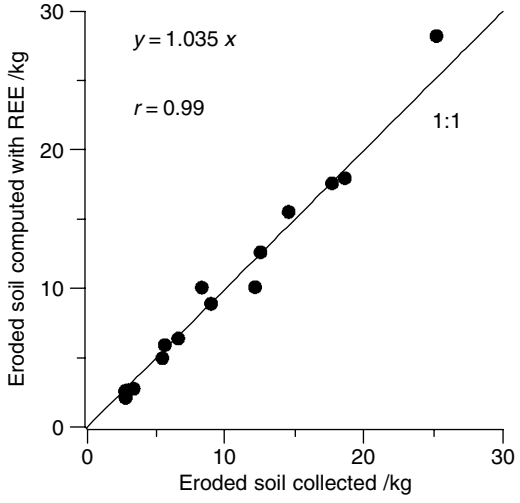


**Figure 4** Comparison of the total eroded soil as measured and that recovered with REE tracing.

## Conclusions

A tracing method using REEs was used to study the dynamic process of rill erosion in laboratory flumes to quantify the erosion process along eroding rills, for better understanding of the spatial variation of rill erosion. Experimental data indicate that sediment concentration increased with rill length under different hydraulic conditions, but the increased rate (the slope of the curve) diminished gradually, and the sediment concentration eventually approached a constant value. The slope gradients had a greater effect on sediment concentration than did flow rate, and a greater flow rate caused heavier rill erosion and soil loss under the same slope gradient. The REE tracing method demonstrated good measurement precision.

The REE tracing technique for rill erosion dynamics has the ability to reveal spatially distributed data which supply insights into rill erosion processes, something that has not been possible with traditional erosion measurement methods. Unlike the method with different rill lengths, the REE method traces the rill erosion under real dynamic situations with continuous flow.

The results indicate that the new methodology developed here is promising and provides a useful tool to further our understanding of rill and soil erosion processes and dynamics.

## Acknowledgements

This paper is based on work supported by the Ministry of Education of China under Project No ZD-0110 and by the Knowledge Innovation Project of CAS, under Grant No KZCX3-SW-42. Thanks to Mr Baoji Wang and Ms Yongcui Yuan from China Agricultural University Library for their services in the literature search.

## References

Abrahams, A.D., Parsons, A.J. & Luk, S.H. 1986. Field measurement of the velocity of overland flow using dye tracing. *Earth Surface Processes and Landforms*, **11,** 653–657.

Huang, C.H., Bradford, J.M. & Laflen, J.M. 1996. Evaluation of the detachment–transport coupling concept in the WEPP rill erosion equation. *Soil Science Society of America Journal*, **60,** 734–739.

Lei, T.W. & Nearing, M.A. 2000. Flume experiments for determining rill hydraulic characteristics, erosion and rill patterns. *Journal of Hydraulic Engineering*, **11,** 49–54.

Lei, T.W., Nearing, M.A., Haghighi, K. & Bralts, V.F. 1998. Rill erosion and morphological evolution: a simulation model. *Water Resources Research*, **34,** 3157–3168.

Lei, T.W., Zhang, Q.W., Zhao, J. & Tang, Z.J. 2001. A laboratory study of sediment transport capacity in the dynamic process of rill erosion. *Transactions of the American Society of Agricultural Engineers*, **44,** 1537–1542.

Lei, T.W., Zhang, Q.W., Zhao, J., Xia, W.S. & Pan, Y.H. 2002. Soil detachment rates for sediment loaded flow in rills. *Transactions of the American Society of Agricultural Engineers*, **45,** 1897–1903.

Merten, G.H., Nearing, M.A. & Borges, A.L.O. 2001. Effect of sediment load on soil detachment and deposition in rills. *Soil Science Society of America Journal*, **65,** 861–868.

Plante, A.F., Duke, M.J.M. & McGill, W.B. 1999. A tracer sphere detectable by neutron activation for soil aggregation and translocation studies. *Soil Science Society of America Journal*, **63,** 1284–1290.

Polyakov, V.O. & Nearing, M.A. 2004. Rare earth element oxides for tracing sediment movement. *Catena*, **55,** 255–276.

Polyakov, V.O., Nearing, M.A. & Shipitalo, M.J. 2004. Tracking sediment redistribution in a small watershed: Implications for agro-landscape evolution. *Earth Surface Processes and Landforms*, **29,** 1275–1291.

Riebe, B. 1995. Monitoring the translocation of soil particles using a neutron activated tracer. In: *Soil Structure: Its Development and Function* (eds K.H. Hartge & B.A. Stewart), pp. 277–297. CRC Press, Boca Raton, FL.

Ritchie, J.C. & McHenry, J.R. 1990. Application of radioactive fallout Cesium-137 for measuring soil erosion and sediment accumulation rates and patterns: a review. *Journal of Environmental Quality*, **19,** 215–233.

Tang, K.L. 2004. *Soil and Water Conservation in China*. Science Press, Beijing (in Chinese).

Tian, J.L. 1997. A primary report for a study on deposition of erosion sediment on slope. *Research on Soil and Water Conservation*, **4,** 57–63 (in Chinese).

Tian, J.L., Zhou, P.H., Liu, P.L. & Wu, P.T. 1992. A preliminary report of REE tracer method for soil erosion. *Journal of Soil and Water Conservation*, **6,** 23–27 (in Chinese).

Toth, S.J. & Alderfer, R.B. 1960. A procedure for tagging water-stable soil aggregates with Co-60. *Soil Science*, **89,** 36–37.

Wallbrink, P.J. & Murray, A.S. 1993. Use of fallout radionuclides as indicators of erosion processes. *Hydrological Processes*, **7,** 297–304.

Walling, D.E. & Quine, T.A. 1990. Calibration of Cesium-137 measurements to provide quantitative erosion rate data. *Land Degradation and Rehabilitation*, **2,** 161–175.

Walling, D.E. & He, Q. 1999. Improved models for estimating soil erosion rates from cesium-137 measurements. *Journal of Environmental Quality*, **28,** 611–622.

Wooldridge, D.D. 1965. Tracing soil particle movement with Fe-59. *Soil Science Society of America Journal*, **29,** 469–472.

Zhang, X.C., Friedrich, J.M., Nearing, M.A. & Norton, L.D. 2001. Potential use of rare earth oxides as tracers for soil erosion and aggregation studies. *Soil Science Society of America Journal*, **65,** 1508–1515.

Zhang, X.C., Nearing, M.A., Polyakov, V.O. & Friedrich, J.M. 2003. Using rare earth oxide tracers for studying soil erosion dynamics. *Soil Science Society of America Journal*, **67,** 279–288.